Planet. Space Sci., Vol. 37, No. 9, pp. 1037–1046, 1989
Printed in Great Britain.

0032-0633/89 $3.00 + 0.00
Pergamon Press plc

A SOLUTION OF THE CHAPMAN–FERRARO PROBLEM FOR AN ELLIPSOIDAL MAGNETOPAUSE

N. A. TSYGANENKO
Institute of Physics, Leningrad State University, Stary Petergof 198904, Leningrad, U.S.S.R.

(*Received* 3 *November* 1988)

Abstract—A simple polynomial expansion for the components of the magnetic field from the magnetospheric surface currents is derived, based on a solution of the boundary problem for a tilted magnetic dipole field confined within an axially symmetric oblong ellipsoidal cavity. The ellipsoidal representation of the magnetospheric boundary is in excellent agreement with its observed shape up to tailward distances of 30–40R_E. The obtained representation of the boundary field can be easily adjusted to arbitrary values of the solar wind ram pressure by means of a simple scaling. A comparison with a paraboloid model is performed, using the fact that the paraboloidal surface can be obtained as a limiting case of the ellipsoidal one by a special choice of its parameters.

1. INTRODUCTION

The problem of shielding the geodipole field by the currents flowing at the boundary of the magnetospheric cavity was studied by many authors, including the first classical works by Chapman and Ferraro (1930, 1931). Some of them solved the problem self-consistently (Mead and Beard, 1964; Choe *et al.*, 1973; Olson, 1969), that is, not only the boundary shielding field, but also the shape of the boundary itself was found, satisfying at any point the condition of the balance between the solar wind ram pressure and electrodynamic stresses in the magnetopause current layer, represented equivalently in terms of the interior magnetic pressure. In an alternative approach developed by Alekseev and Shabansky (1972), Voigt (1972) and Tsyganenko (1976), the magnetopause is treated as a surface with a given shape providing reasonable agreement with the observed one, and the boundary magnetic field distribution is computed from the requirement of complete or partial (Voigt, 1981) shielding of intra-magnetospheric sources outside the cavity.

The models designed for practical calculations should also meet the requirements of (i) a relative simplicity of mathematical representation of the magnetic field components as well as (ii) a sufficiently extended region of validity of the model. Besides that, it is necessary that (iii) the model be capable of taking into account in a simple way changes in the solar wind momentum flux leading to variations of the magnetospheric dimensions.

In the well-known model by Mead (1964) generalized later by Choe *et al.* (1973) to the case of nonzero dipole tilt angle [corrected by Halderson *et al.* (1975)] the boundary field is approximated by a spherical harmonic expansion containing positive powers of the radial geocentric distance r. Unfortunately, such a series yields satisfactory results only within a limited near-Earth region and becomes completely inappropriate for $r \gtrsim 10R_E$, due to a poor convergence. This motivated Beard *et al.* (1982) to propose a separate representation of the boundary field in the magnetotail by means of cylindrical harmonics. However, these results have not been extended to the case of tilted geodipole. Some difficulties arise also in this approach in relation to the problem of matching the solutions pertaining to two separate modeling regions.

A comparatively simple representation of the boundary current field is provided by a model with the paraboloid shape of the magnetopause, first proposed by Alekseev and Shabansky (1972) and considerably developed in a recent paper by Stern (1985). The paraboloid surface shows a good agreement with the observed magnetopause at the dayside, but expands too rapidly in the tailward region (a perturbation method for modification of the parabolic harmonic expansion to the case of non-paraboloid boundaries was proposed in this relation by Stern in the above cited work). Besides that, the paraboloid model requires computation of the ordinary (J_0, J_1) and mofidifed (I_0, I_1) Bessel functions, which are not always convenient in practice.

In the present work a similar problem is solved for a cavity having the shape of an oblong ellipsoid of revolution. In the front magnetospheric region $X_{GSM} \gtrsim -30R_E$ the ellipsoid provides an excellent approximation to the observed magnetopause. At larger distances the ellipsoid surface tapers down and

closes; however, contributions from both the geodipole and boundary sources do not exceed a few tenths of nanotesla in this region, at least an order of magnitude less than that from the tail current sheet. Therefore, the ellipsoid model for the dipole shielding field can actually be used up to its rear boundary, which may be placed at distances of the order of lunar orbit radius or even farther. The main advantage of the model consists in that the obtained mathematical representation appears to be rather simple and can be reduced to the polynomials of the solar magnetospheric Cartesian coordinates, which are easily adjustable to a given value of the solar wind momentum flux.

2. TRANSFORMATION TO ELLIPSOIDAL COORDINATES

Consider a cavity having a shape of an oblong ellipsoid of revolution (Fig. 1) with both its foci lying at the X axis of the solar–magnetospheric coordinate system (GSM) and spaced by the distance $2a$. The front focus is located at $X_{GSM} = X_0$. Let us introduce the ellipsoidal coordinates (σ, τ, φ) [see Chapter 6, Table 6 of Korn and Korn (1961)], related to the solar–magnetospheric ones (x, y, z) by the following transformation

$$\sigma = \frac{1}{a}\left[\frac{s^2+(s^4-4a^2x'^2)^{1/2}}{2}\right]^{1/2}$$

$$\tau = \frac{1}{a}\left[\frac{s^2-(s^4-4a^2x'^2)^{1/2}}{2}\right]^{1/2} \text{sign}\,(x')$$

$$\varphi = \tan^{-1}(z/y), \tag{1}$$

where $x' = x - x_0 + a$ and $s^2 = a^2 + x'^2 + y^2 + z^2$.

The inverse transformation reads as follows:

$$x = x_0 - a(1-\sigma\tau)$$

$$y = a(\sigma^2-1)^{1/2}(1-\tau^2)^{1/2}\cos\varphi$$

$$z = a(\sigma^2-1)^{1/2}(1-\tau^2)^{1/2}\sin\varphi. \tag{2}$$

Figure 1 shows contours of constant σ and τ in the plane $y = 0$. The interior of ellipsoidal cavity corresponds to the intervals of coordinates $1 \leqslant \sigma \leqslant \sigma_0$, $-1 \leqslant \tau \leqslant 1$, $0 \leqslant \varphi < 2\pi$. The magnetopause shape and location is defined completely by setting the values of the parameters x_0, a, and σ_0. The subsolar point distance and the radius of the dawn–dusk cross-section are, respectively,

$$r_S = x_0 + a(\sigma_0 - 1)$$

$$r_D = [r_S(1-\sigma_0^{-2})(2a\sigma_0 - r_S)]^{1/2}. \tag{3}$$

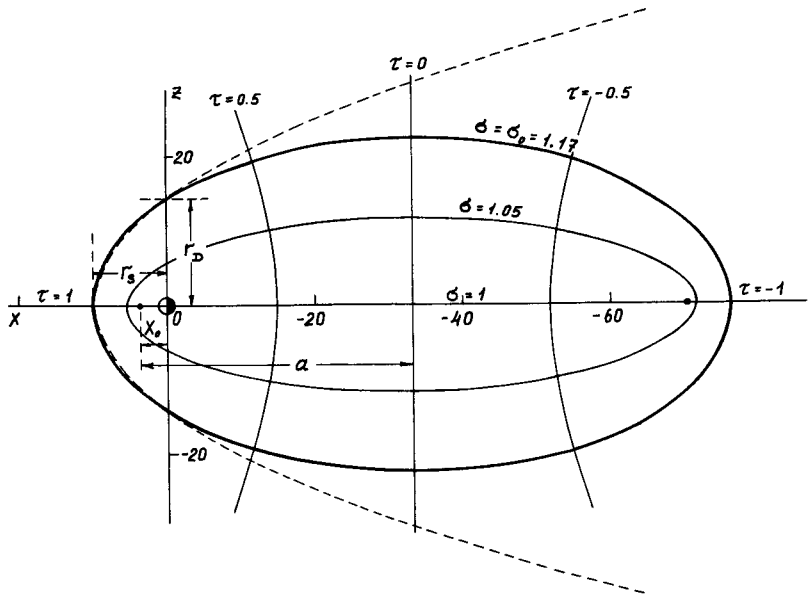

FIG. 1. CONTOURS OF CONSTANT ELLIPSOIDAL COORDINATES σ AND τ IN THE GSM MIDDAY–MIDNIGHT MERIDIAN PLANE.

The ellipsoid with $\sigma = \sigma_0 = 1.17$ represents the magnetopause with the subsolar point at $x = r_S = 10R_E$ and $r_D = 14.366R_E$. The front focus lies at $x_0 = 3.71$, and $a = 37R_E$. The dashed line corresponds to the paraboloid with the same r_S and r_D.

The points lying at the x axis are given by the following intervals of ellipsoidal coordinates: (i) $\tau = 1$ and $1 \leqslant \sigma \leqslant \sigma_0$, (ii) $-1 \leqslant \tau \leqslant 1$ and $\sigma = 1$, (iii) $\tau = -1$ and $1 \leqslant \sigma \leqslant \sigma_0$, which correspond to (i) $x_0 \leqslant x \leqslant r_S$, (ii) $x_0 - 2a \leqslant x \leqslant x_0$, and (iii) $2(x_0 - a) - r_S \leqslant x \leqslant x_0 - 2a$.

The following relations also hold, which will be used later on:

$$\sigma\tau = x'/a$$
$$\sigma^2 + \tau^2 = 1 + (x'^2 + \rho^2)/a^2$$
$$(\sigma^2 - 1)^{1/2}(1 - \tau^2)^{1/2} = \rho/a, \tag{4}$$

where $\rho^2 = y^2 + z^2$.

A search for appropriate values of the ellipsoid parameters gave the following ones: $x_0 = 3.71R_E$, $a = 37R_E$, and $\sigma_0 = 1.17$, yielding a good agreement with the average observed magnetopause shape (Fairfield, 1971). Being substituted in (3), these values give $r_S = 10R_E$ and $r_D = 14.366R_E$. The maximal radius of the cavity (minor semiaxis) equals $r_M = a(\sigma_0^2 - 1)^{1/2} \simeq 22.47R_E$ at $x = x_0 - a = -33.3R_E$.

3. EXPANSIONS FOR THE POTENTIAL OF THE MAGNETIC FIELD FROM THE BOUNDARY SOURCES

Following the standard formulation of the Chapman–Ferraro problem for a magnetospheric cavity of a given shape (e.g. Alekseev and Shabansky, 1972) and using the notations by Stern (1985), we arrive at the Neumann's boundary problem

$$\Delta\gamma_{0,1} = 0$$
$$\left.\frac{\partial\gamma_{0,1}}{\partial\sigma}\right|_{\sigma=\sigma_0} = -\left.\frac{\partial\gamma_{d0,1}}{\partial\sigma}\right|_{\sigma=\sigma_0} = F_{0,1}(\tau, \varphi). \tag{5}$$

Here γ_0 and γ_1 are the scalar potentials for the shielding field from the magnetopause currents, which correspond, respectively, to the parallel and perpendicular orientation of the dipole of unit magnetic moment. The functions F_0 and F_1 in the boundary condition represent the normal components of the dipole magnetic field at the boundary, obtained as the negative derivatives of the dipole potentials γ_{d0} and γ_{d1}. The final solution can be expressed in terms of γ_0 and γ_1 as (Alekseev and Shabansky, 1972; Stern, 1985)

$$\gamma = g(\gamma_0 \sin\psi + \gamma_1 \cos\psi), \tag{6}$$

where ψ is the tilt angle of the geodipole axis with respect to the z_{GSM} one, and g is the Earth's magnetic moment. For the epoch 1980.0 the value of $g = -30574\ \mathrm{nT} \times R_E^3$ should be taken.

The Laplace's equation in (5) reads in ellipsoidal coordinates as (Korn and Korn, 1961)

$$\frac{\partial}{\partial\sigma}\left[(\sigma^2 - 1)\frac{\partial\gamma}{\partial\sigma}\right] + \frac{\partial}{\partial\tau}\left[(1 - \tau^2)\frac{\partial\gamma}{\partial\tau}\right] + \frac{\sigma^2 - \tau^2}{(\sigma^2 - 1)(1 - \tau^2)}\frac{\partial^2\gamma}{\partial\varphi} = 0.$$

Its general solution can be obtained by separating the variables in a standard way, with the result in a form of expansion:

$$\gamma = \sum_{n=1}^{\infty}\sum_{m=0}^{n} \mathrm{P}_n^m(\sigma)\mathrm{P}_n^m(\tau)(a_{nm}\cos m\varphi + b_{nm}\sin m\varphi) \tag{7}$$

containing the associate Legendre functions of the first kind.

The dipole potentials have the form

$$\gamma_{d0} = x/R^3 \quad \text{and} \quad \gamma_{d1} = z/R^3,$$

from which the right-hand sides of the boundary conditions in (5) follow as

$$F_0 = (a/R^3)\{\tau - 3(x_0 - a + a\sigma_0\tau) \times [a\sigma_0 + \tau(x_0 - a)]/R^2\} \equiv f_0(\tau) \tag{8}$$

$$F_1 = (a/R^3)[(\sigma_0^2 - 1)(1 - \tau^2)]^{1/2}\{\sigma_0/(\sigma_0^2 - 1) - (3a/R^2)[a\sigma_0 + \tau(x_0 - a)]\} \times \sin\varphi \equiv f_1(\tau)\sin\varphi \tag{9}$$

where

$$R^2 = x^2 + y^2 + z^2 = a^2(\sigma_0^2 + \tau^2) + 2a(x_0 - a)\sigma_0\tau + x_0(x_0 - 2a).$$

As is seen from (8), the boundary condition for γ_0 does not contain any φ-dependence due to axial symmetry of the shielding field for the x-aligned dipole. The function F_1 for the z-aligned dipole orientation depends on φ only through the factor $\sin\varphi$. By this reason, the expansion (7) is reduced in these particular cases to a more simple form, containing the summation over n only. Truncating this infinite series to the leading N terms, we obtain

$$\gamma_0 = \sum_{n=1}^{N} a_{0n}\mathrm{P}_n(\sigma)\mathrm{P}_n(\tau) \tag{10}$$

$$\gamma_1 = \sum_{n=1}^{N} a_{1n}\mathrm{P}_n^1(\sigma)\mathrm{P}_n^1(\tau)\sin\varphi. \tag{11}$$

Using the boundary conditions (8) and (9) and orthogonality of the Legendre functions, the coefficients in (10) and (11) can be found as

$$a_{0n} = (n + \tfrac{1}{2})/\mathrm{P}_n'(\sigma_0)\int_{-1}^{1} f_0(\tau)\mathrm{P}_n(\tau)\,\mathrm{d}\tau \tag{12}$$

$$a_{1n} = (n+\tfrac{1}{2})/[n(n+1)\mathrm{P}_n^1{}'(\sigma_0)] \times \int_{-1}^{1} f_1(\tau)\mathrm{P}_n^1(\tau)\,\mathrm{d}\tau. \quad (13)$$

Note also that, since $\sigma \geqslant 1$, the associate functions $\mathrm{P}_n^1(\sigma)$ should be calculated as $\mathrm{P}_n^1(\sigma) = \sqrt{\sigma^2-1}\,\mathrm{P}_n'(\sigma)$ (Abramowitz and Stegun, 1964).

The first 20 coefficients computed from (12) and (13) for the above specified values of the ellipsoid parameters are listed in Table 1.

4. THE MAGNETIC FIELD COMPONENTS

Calculating the minus gradient of the potential yields the magnetic field vectors $\mathbf{b}_{0,1}$, corresponding to the parallel and perpendicular dipoles of unit strength

$$\mathbf{b}_{0,1} = -\nabla\gamma_{0,1}(\sigma,\tau,\varphi) = -\frac{\partial\gamma_{0,1}}{\partial\sigma}\nabla\sigma - \frac{\partial\gamma_{0,1}}{\partial\tau}\nabla\tau - \frac{\partial\gamma_{0,1}}{\partial\varphi}\nabla\varphi.$$

Using (1) and (2) then gives in components

$$b_{x_{0,1}} = -\frac{1}{a(\sigma^2-\tau^2)}\left[\tau(\sigma^2-1)\frac{\partial\gamma_{0,1}}{\partial\sigma} + \sigma(1-\tau^2)\frac{\partial\gamma_{0,1}}{\partial\tau}\right] \quad (14)$$

$$b_{\{y/z\}_{0,1}} = \frac{[(\sigma^2-1)(1-\tau^2)]^{1/2}}{a(\sigma^2-\tau^2)}\left(\tau\frac{\partial\gamma_{0,1}}{\partial\tau} - \sigma\frac{\partial\gamma_{0,1}}{\partial\sigma}\right) \times \begin{Bmatrix}\cos\varphi\\ \sin\varphi\end{Bmatrix} + \frac{1}{a[(\sigma^2-1)(1-\tau^2)]^{1/2}}\frac{\partial\gamma_{0,1}}{\partial\varphi} \times \begin{Bmatrix}\sin\varphi\\ -\cos\varphi\end{Bmatrix}. \quad (15)$$

Inserting the truncated expansions (10) and (11) in (14) and (15) gives the final expressions for calculating the magnetic field components. However, since (14) and (15) contain indeterminacies at the ellipsoid foci ($\sigma = 1$ and $\tau = \pm 1$), an additional treatment at the level of separate expansion terms is necessary, in order to make the expressions manageable for practical calculations.

Let us consider first the x-component for the case of parallel dipole shielding. Substituting in (14) the terms of the expansion (10) and eliminating the derivatives of the Legendre functions by means of known relationships (Abramowitz and Stegun, 1964) we obtain

$$b_{x_0} = -\frac{1}{a(\sigma^2-\tau^2)}\sum_{n=1}^{N} a_{0n}n\{\sigma\mathrm{P}_n(\sigma)\mathrm{P}_{n-1}(\tau) - \tau\mathrm{P}_n(\tau)\mathrm{P}_{n-1}(\sigma)\}. \quad (16)$$

It can easily be shown that for any n the expression in curly brackets may be written as

$$(\sigma^2 \mp \tau^2)A_{K_n}(t,v)(\sigma\tau)^{l_n}.$$

Here $A_{K_n}(t,v)$ is a polynomial of two variables, $t = \sigma^2\tau^2 = (x'/a)^2$ and $v = \sigma^2+\tau^2 = (a^2+\rho^2+x'^2)/a^2$, of degree $K_n = [(n-1)/2]$, where the square brackets denote the biggest integer of the inside quantity and the power l_n equals 0 for odd and 1 for even values of n. As a result of summation, (16) can be reduced to the form

$$b_{x_0} = R_{M_N}(t,v,x') = R_{M_N}^{(1)}(t,v) + (x'/a)R_{M_N}^{(2)}(t,v) \quad (17)$$

where $R_{M_N}^{(1)}$ and $R_{M_N}^{(2)}$ are polynomials of t and v, and of degree $M_N = [(N-1)/2]$.

Quite similarly, using (4), all other components are derived as

$$b_{x_1} = (z/a)S_{M_N} = (z/a)\{S_{M_N}^{(1)}(t,v) + (x'/a)S_{M_N}^{(2)}(t,v)\} \quad (18)$$

TABLE 1. COEFFICIENTS FOR THE LEADING TWENTY TERMS IN THE EXPANSIONS (10) AND (11) FOR THE PARALLEL (a_{0n}) AND PERPENDICULAR (a_{1n}) DIPOLE SHIELDING POTENTIAL INSIDE THE ELLIPSOID WITH $x_0 = 3.71$, $a = 37$, AND $\sigma_0 = 1.17$

n	a_{0n}	a_{1n}	n	a_{0n}	a_{1n}
1	4.160E-3	2.997E-3	11	−9.895E-7	−8.831E-9
2	3.486E-3	8.793E-4	12	−3.533E-4	−2.635E-9
3	2.089E-3	2.579E-4	13	−1.007E-7	−6.368E-10
4	9.911E-4	7.043E-5	14	−2.000E-8	−1.086E-10
5	3.829E-4	1.739E-5	15	−2.873E-10	−1.354E-12
6	1.175E-4	3.677E-6	16	2.223E-9	9.175E-12
7	2.461E-5	5.599E-7	17	1.412E-9	5.147E-12
8	−1.152E-8	−1.988E-10	18	6.096E-10	1.976E-12
9	−3.373E-6	−4.559E-8	19	2.096E-10	6.084E-13
10	−2.206E-6	−2.398E-8	20	5.765E-11	1.507E-13

$$b_{\{y_0/z_0\}} = \begin{Bmatrix}(y/a)\\(z/a)\end{Bmatrix} \times \{T^{(1)}_{M_N}(t,v) + (x'/a)T^{(2)}_{M_N}(t,v)\} \quad (19)$$

$$b_{y_1} = (yz/a^2)\{U^{(1)}_{M_N}(t,v) + (x'/a)U^{(2)}_{M_N}(t,v)\} \quad (20)$$

$$b_{z_1} = (z^2/a^2)\{U^{(1)}_{M_N}(t,v) + (x'/a)U^{(2)}_{M_N}(t,v)\} - \{V^{(1)}_{M_N}(t,v) + (x'/a)V^{(2)}_{M_N}(t,v)\}. \quad (21)$$

Coefficients of the polynomials R, S, T, U, V in (17)–(21) include a combination of the coefficients a_{0n} or a_{1n} from Table 1 and those of Legendre functions; their concrete values depend on the length N of truncated expansions (10) and (11) for the potentials and will be given in the next section.

After the components of **b** are found from (17)–(21), the full vector **B** can be obtained as a linear combination of $\mathbf{b}_0$ and $\mathbf{b}_1$ with the weight factors $g\sin\psi$ and $g\cos\psi$, in quite a similar way, as for the potential in (6).

In addition, it is worth noting that the same polynomial representation (17)–(21) for the field components could be obtained in a slightly shorter and straightforward way, if the truncated expansions for the potentials (10) and (11) were reduced to the polynomials in Cartesian coordinates similar to R–V ones in (17)–(21), subsequently taking derivatives of x, y, and z.

5. NUMERICAL RESULTS

To elucidate the question on the optimal length of the truncated expansions providing an adequate accuracy of the shielding field representation, the values of the derivatives $\partial\gamma_{0,1}/\partial\sigma$ were computed in several boundary points for different numbers of terms in the expansions. In the case of an ideally accurate perfect shielding these values should equal the derivatives of the dipole potentials $\partial\gamma_{d0,1}/\partial\sigma$ evaluated at the same locations. Table 2, similar in its structure to that in the paper by Stern (1985) for the paraboloid model, represents the results of comparison of the derivatives for ten values of x coordinate within the range $-70 \leqslant x \leqslant 6R_E$ and for three different expansion lengths, $N = 20$, 10 and 6. In the first case with $N = 20$, the boundary normal component of the dipole field is shielded by the magnetopause sources within the accuracy of 1–2%, the best results being observed for the front magnetopause region with $x \gtrsim -30R_E$, where the discrepancies do not exceed 0.2%. Figure 2 shows the magnetic field lines of the tilted geodipole completely shielded by the boundary field, calculated by means of a direct numerical differentiation of the potential (10) and (11) with $N = 20$.

For shorter expansions the discrepancies are larger,

TABLE 2. BOUNDARY VALUES OF $\partial\gamma_0/\partial\sigma$ AND $\partial\gamma_1/\partial\sigma$ AS OBTAINED BY SUMMATION OVER FIRST N TERMS OF EXPANSIONS (10) AND (11) FOR THE SHIELDING POTENTIALS, IN COMPARISON WITH THE CORRESPONDING VALUES FOR PARALLEL (d_0) AND PERPENDICULAR (d_1) DIPOLES, AT DIFFERENT LOCAL x

		$\partial\gamma_0/\partial\sigma$				$\partial\gamma_1/\partial\sigma$			
τ	x	$-\partial\gamma_{d0}/\partial\sigma$	$N=20$	$N=10$	$N=6$	$-\partial\gamma_{d1}/\partial\sigma$	$N=20$	$N=10$	$N=6$
0.9	5.7	2.220E-2	2.220E-2	2.217E-2	2.225E-2	5.659E-2	5.658E-2	5.503E-2	5.309E-2
0.7	−3.0	−1.167E-2	−1.167E-2	−1.247E-2	−1.232E-2	1.901E-2	1.901E-2	1.941E-2	2.178E-2
0.5	−11.6	−7.325E-3	−7.323E-3	−6.806E-3	−8.604E-3	4.301E-3	4.301E-3	3.909E-3	2.562E-3
0.3	−20.3	−3.776E-3	−3.776E-3	−3.937E-3	−2.377E-3	8.901E-4	8.877E-4	1.412E-3	9.410E-7
0.1	−29.0	−2.035E-3	−2.037E-3	−2.241E-3	−1.367E-3	6.473E-5	6.551E-5	−3.469E-4	1.462E-3
−0.1	−37.6	−1.169E-3	−1.167E-3	−7.917E-4	−2.236E-3	−1.253E-4	−1.239E-4	−5.577E-5	6.491E-4
−0.3	−46.3	−7.094E-4	−7.086E-4	−9.855E-4	−1.369E-3	−1.451E-4	−1.468E-4	1.060E-4	−1.244E-3
−0.5	−54.9	−4.501E-4	−4.516E-4	−3.870E-4	5.281E-4	−1.192E-4	−1.201E-4	−4.925E-4	−8.550E-4
−0.7	−63.6	−2.955E-4	−2.972E-4	−2.397E-4	1.572E-5	−8.266E-5	−8.182E-5	2.977E-4	1.207E-5
−0.9	−72.3	−1.992E-4	−2.010E-4	1.487E-5	−1.298E-3	−4.150E-5	−4.276E-5	−4.676E-4	−9.128E-4

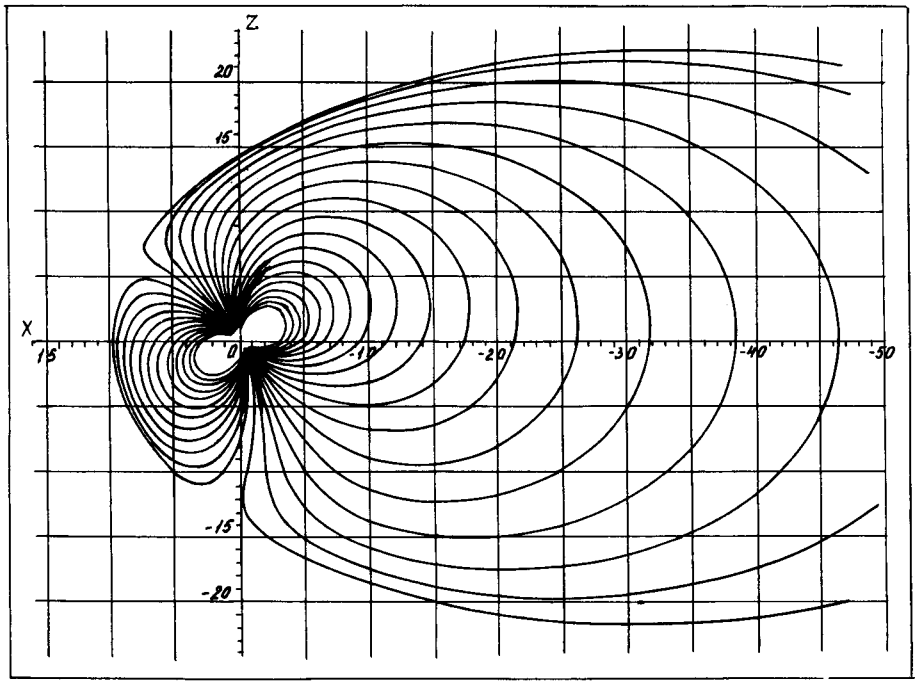

FIG. 2. MAGNETIC FIELD LINE CONFIGURATION OBTAINED FOR THE TILTED DIPOLE FIELD ($\psi = 30°$) CONFINED WITHIN THE ELLIPSOIDAL CAVITY OF FIG. 1.
The boundary current field was computed from (10) and (11) with $N = 20$, by means of numerical computation of the $-\nabla\gamma$ components. Field lines start from Earth's Northern Hemisphere at latitudes 2° apart, beginning from 60°.

the most significant deviations arising in the rear part of the ellipsoidal boundary, so that the region of satisfactory field representation shrinks towards the subsolar magnetospheric domain. Nevertheless, even relatively short sums yield sufficiently good results within distances $R \lesssim R_E$, which can be seen from Figs 3 and 4 showing the field line configurations obtained from the polynomial representation (17)–(21) with $N = 10$ and 6, respectively. In these two cases the polynomials R, S, T. U, V have the degree $M_{10} = 4$ and $M_6 = 2$. Tables 3 and 4 give the values of coefficients for these polynomials along with the explicit form of the corresponding terms.

6. SCALING AND COMPARISON WITH THE PARABOLOID MODEL

Variations of the solar wind dynamical ram pressure $P_d = nmV^2$ cause the changes in the location of the magnetospheric boundary. An important feature is that the geocentric distance to any point of the magnetopause with constant angular coordinates (as viewed from the dipole location) changes in approximately the same proportion. In other words, the magnetopause shrinks and expands nearly self-similarly with respect to the origin. This was first shown by Mead and Beard (1964) and stems, in fact, from the self-similarity of the dipole field.

Therefore, to take into account a change in the solar wind ram pressure from a "standard" value P_{d_0} up to a currently observed one P_d, we have to multiply the parameters a and x_0 by a factor K and to retain the parameter σ_0 by the same value. As can be seen from (3), the characteristic distances r_S and r_D also change by the factor K after the scaling. All the coefficients, as follows from (12) and (13), acquire the factor K^{-2} and, therefore, the magnetic field components scale by K^{-3} at any point with a fixed value of (σ, τ, φ). The last scaling factor holds also for the dipole field components at points with constant coordinates (σ, τ, φ) and hence the same is true for the total field. At the magnetopause, where $\sigma = \sigma_0$, the points with $\tau =$ constant correspond to the constant angles of incidence of the solar wind, for any value of P_d, and thus the scaling procedure becomes consistent with

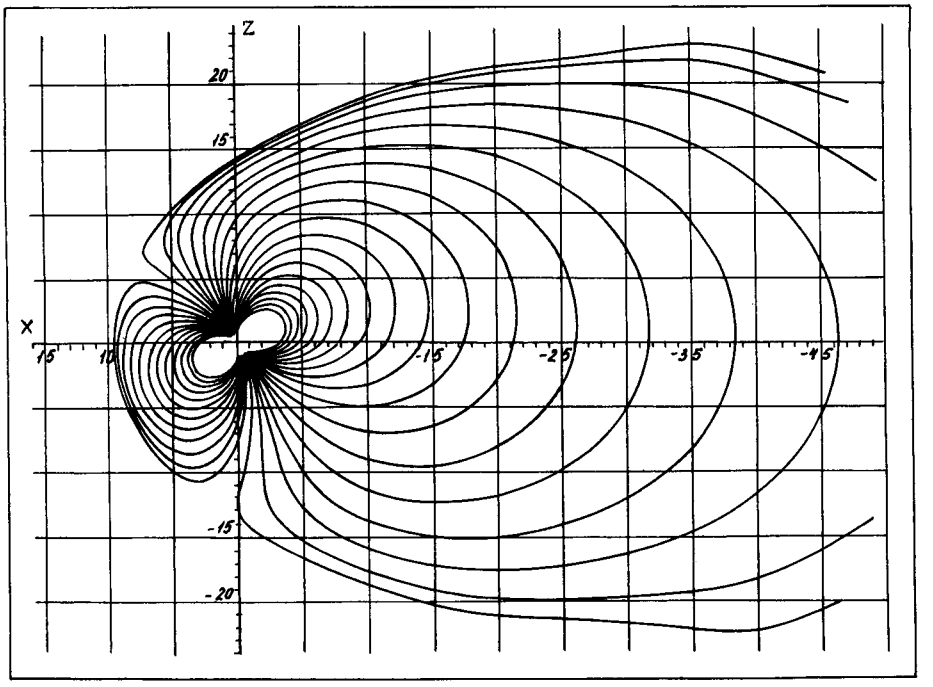

FIG. 3. MAGNETIC FIELD LINE CONFIGURATION SIMILAR TO THAT SHOWN IN FIG. 2, COMPUTED USING THE POLYNOMIAL REPRESENTATION OF THE SHIELDING FIELD COMPONENTS (17)–(21) WITH $N = 10$.

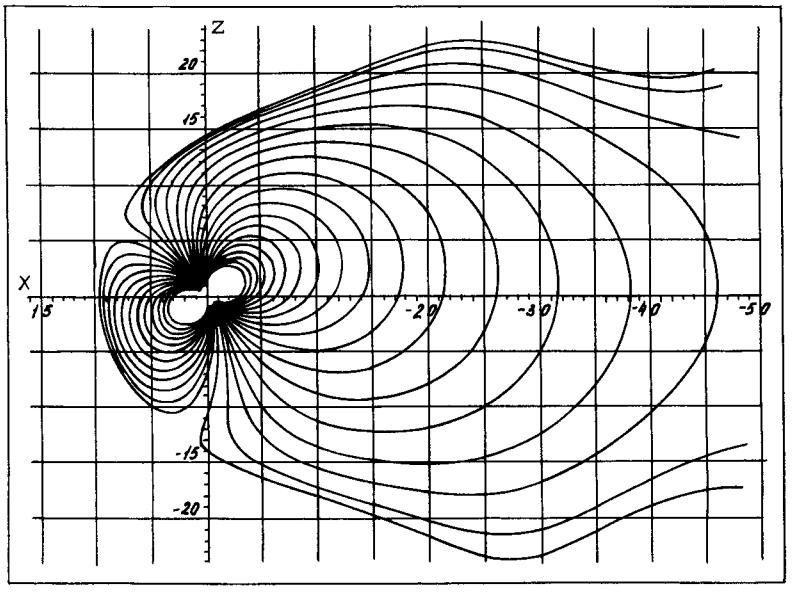

FIG. 4. SIMILAR TO FIG. 3, WITH $N = 6$.

TABLE 3. COEFFICIENTS OF THE POLYNOMIALS R, S, T, U, V IN (17)–(21) FOR $N = 10$. The corresponding terms are given in the first column, where $t = (\sigma\tau)^2 = (x'/a)^2$, $v = \sigma^2+\tau^2 = (a^2+x'^2+y^2+z^2)/a^2$, $\xi = x'/a$. Blank positions correspond to zero coefficients

Term	R	S	T	U	V
t^4	3.9169E-3	1.0993E-2	−9.1937E-3		−9.0000E-4
t^3v	−7.3115E-3	−1.8107E-2	1.5143E-2		1.4824E-3
t^2v^2	4.2182E-3	9.0553E-3	−7.5713E-3		−7.4118E-4
tv^3	−7.6694E-4	−1.3928E-3	1.1648E-3		1.1403E-4
v^4	2.1304E-5	3.1655E-5	−2.6473E-5		−2.5915E-6
t^3	3.6565E-3	1.2392E-2	−1.0364E-2	−2.9674E-3	−4.2611E-4
t^2v	−3.4522E-3	−1.1513E-2	9.6284E-3	2.9647E-3	2.6361E-4
tv^2	6.3945E-4	2.3803E-3	−1.9906E-3	−6.8416E-4	−9.6960E-6
v^3	−6.1025E-6	−6.0020E-5	5.0194E-5	2.0732E-5	−1.9445E-6
t^2	−1.6378E-3	1.0736E-3	−1.0768E-3	−5.2721E-4	8.6294E-4
tv	1.7692E-3	3.4214E-4	−1.6681E-4	3.8784E-5	−5.7961E-4
v^2	−1.8424E-4	−7.5884E-5	5.4938E-5	1.1667E-5	3.9734E-5
t	−1.9431E-3	−2.0250E-3	1.4549E-3	1.1592E-3	6.7481E-4
v	4.0205E-4	3.4430E-4	−2.4703E-4	−1.5893E-4	−1.0318E-4
1	−2.7848E-4	−3.3760E-4	2.2929E-4	2.0635E-4	9.8400E-5
$t^4\xi$	1.0215E-2				−2.1098E-3
$t^3v\xi$	−2.1632E-2				3.9975E-3
$t^2v^2\xi$	1.5143E-2				−2.4691E-3
$tv^3\xi$	−3.8827E-3				5.4868E-4
$v^4\xi$	2.6473E-4				−3.1655E-5
$t^3\xi$	1.6171E-2	4.2353E-3	−3.4817E-3	−7.9951E-3	−2.6370E-3
$t^2v\xi$	−2.1462E-2	−5.9294E-3	4.8743E-3	9.8763E-3	3.0334E-3
$tv^2\xi$	7.6378E-3	2.2805E-3	−1.8747E-3	−3.2921E-3	−9.1346E-4
$v^3\xi$	−6.1333E-4	−2.0732E-4	1.7043E-4	2.5324E-4	6.0020E-5
$t^2\xi$	5.1436E-3	2.0294E-3	−1.7415E-3	−6.0668E-3	−1.2864E-4
$tv\xi$	−2.3205E-3	−1.0156E-3	9.0142E-4	3.6538E-3	−2.1522E-4
$v^2\xi$	−2.8465E-5	3.1059E-5	−3.6615E-5	−3.6012E-4	7.5884E-5
$t\xi$	−2.0511E-3	−2.2926E-3	1.6708E-3	4.3045E-4	9.0454E-4
$v\xi$	1.2079E-3	1.0003E-3	−7.3697E-4	−3.0354E-4	−3.4430E-4
ξ	−9.5264E-4	−1.1433E-3	8.0411E-4	6.8860E-4	3.3760E-4

TABLE 4. THIS TABLE IS SIMILAR TO TABLE 3, BUT CONTAINS THE COEFFICIENTS FOR SHORTER EXPANSIONS, CORRESPONDING TO $N = 6$

Term	R	S	T	U	V
t^2	−1.7827E-3	−2.3728E-3	1.8053E-3		7.2868E-4
tv	1.5280E-3	1.5818E-3	−1.2035E-3		−4.8579E-4
v^2	−1.5280E-4	−1.1299E-4	8.5967E-5		3.4699E-5
t	−1.7557E-3	−2.2147E-3	1.6136E-3	9.7158E-4	6.4654E-4
v	3.8151E-4	3.5255E-4	−2.5394E-4	−1.3880E-4	−1.0155E-4
1	−2.7585E-4	−3.3808E-4	2.2969E-4	2.0310E-4	9.8335E-5
$t^2\xi$	−2.1664E-3				7.4572E-4
$tv\xi$	2.4071E-3				−6.7793E-4
$v^2\xi$	−5.1580E-4				1.1299E-4
$t\xi$	−2.9538E-3	−1.9432E-3	1.4262E-3	1.3559E-3	9.7328E-4
$v\xi$	1.3596E-3	8.3278E-4	−6.1122E-4	−4.5195E-4	−3.5255E-4
ξ	−9.6725E-4	−1.0900E-3	7.6301E-4	7.0511E-4	3.3808E-4

the pressure balance condition, if we assume $K = (P_{d_0}/P_d)^{1/6}$.

The model allows a comparison with the paraboloid model by means of a special choice of the ellipsoid parameters. Namely, we have to specify x_0, a, and σ_0 in such a way, that the dependence of the magnetopause radius on x

$$\rho \sim (1-\tau^2)^{1/2} = \{1-[(x-x_0+a)/a\sigma_0]^2\}^{1/2}$$

pertaining to the ellipsoid, converts into a parabolic dependence

$$\rho \sim (1-x/r_S)^{1/2}$$

in the limit of $a \to \infty$, and $|x| \ll a$.

TABLE 5. VALUES OF B_x- AND B_z-COMPONENTS OF THE SHIELDING FIELD FROM BOUNDARY CURRENTS FOR SEVERAL POINTS IN THE $Y = 0$ PLANE.
Each pair of values gives, respectively, B_x and B_z in nanoteslas. Upper values are for the ellipsoidal model and the lower ones (in brackets) are for the paraboloid one with the same $r_S = 10R_E$, and $r_D = 14.366R_E$. This table corresponds to the perpendicular orientation of the geodipole ($\psi = 0$)

z \ x	10	0	−20	$-30R_E$
0	0.0 44.2	0.0 19.5	0.0 3.0	0.0 1.2
	(0.0 42.2)	(0.0 18.9)	(0.0 2.5)	(0.0 1.0)
5		9.0 18.1	1.3 2.8	0.5 1.2
		(9.5 17.6)	(1.2 2.3)	(0.4 0.9)
$10R_E$		17.1 13.5	2.4 2.1	1.0 0.9
		(18.2 12.3)	(2.1 1.7)	(0.8 0.7)

This can be achieved by setting

$$\sigma_0 = (1 - r_D^2/2ar_S)^{-1/2}$$

and

$$x_0 = r_S - r_D^2/4r_S$$

with a sufficiently large value of a.

For carrying out a test computation I took $a = 1000R_E$, $x_0 = 4.8407R_E$, and $\sigma_0 = 1.0052$, which gave the same values of $r_S = 10$ and $r_D = 14.366$, as for the original "reference" ellipsoid with $a = 37$, $x_0 = 3.71$, and $\sigma_0 = 1.17$. Up to tailward distances of $x \sim -100R_E$ the corresponding surface is very close to a paraboloidal one (shown in Fig. 1 by a dashed line). The only difficulty here lies in that the convergence of the expansions (10) and (11) deteriorates by $\sigma_0 \to 1$, which complicates numerical computation of the potentials and magnetic fields. To obtain a satisfactory close agreement between $\partial\gamma_{0,1}/\partial\sigma$ and $-\partial\gamma_{d0,1}/\partial\sigma$ at the "parabolic" boundary up to tailward distances $x \sim -30R_E$, it appeared necessary to take into account $N = 100$ leading terms in (10) and (11).

Table 5 gives the values of B_x- and B_z-components of the boundary field (perpendicular geodipole orientation) in the midday–midnight meridian plane, for both ellipsoidal and nearly paraboloidal shielding surfaces. In the first case the B_z-component values are slightly larger, due to a somewhat tighter confinement of the dipole by the ellipsoidal boundary. In general, the difference is relatively small. In the tailward region both ellipsoidal and paraboloidal shielding field values do not exceed several tenths of a nanotesla. In fact, this allows one to use the obtained representation of the dipole-shielding field up to the rear boundary of the ellipsoid, since small discrepancies arising due to inadequate shape of the model magnetopause are much less than the field from the tail current sheet in this region. At larger tailward distances the expansions (10) and (11) and (17)–(21) diverge and hence become inappropriate.

Finally, a similar representation can in principle be obtained for the boundary field shielding any intramagnetospheric current system. The only restriction here is that the current circuit be completely closed inside the magnetosphere, in order to ensure validity of the scalar potential method.

REFERENCES

Abramowitz, M. and Stegun I. A. (1964) *Handbook of Mathematical Functions.* National Bureau of Standards, Applied Mathematics Series, Washington D.C.

Alekseev, I. I. and Shabansky, V. P. (1972) A model of magnetic field in the geomagnetosphere. *Planet. Space Sci.* **20**, 117.

Beard, D. B., Hirschi, D. and Propp, K. (1982). The tailward magnetopause field beyond $10R_E$. *J geophys Res.* **87**, 2533.

Chapman, S. and Ferraro, V. C. A. (1930) A new theory of magnetic storms. *Nature* **126**, 129.

Chapman, S. and Ferraro, V. C. A. (1931) A new thoery of magnetic storms, 1. The initial phase. *J. geophys. Res.* **36**, 77.

Choe, Y. J., Beard, D. B. and Sullivan, E. C. (1973) Precise calculation of the magnetosphere surface for a tilted dipole. *Planet. Space Sci.* **21**, 485.

Fairfield, D. H. (1971) Average and unusual locations of the Earth's magnetopause and bow shock. *J. geophys. Res.* **76**, 6700.

Halderson, D. W., Beard, D. B. and Choe, J. Y. (1975) Corrections to "The compressed geomagnetic field as a function of dipole tilt". *Planet. Space Sci.* **23**, 887.

Korn, G. A. and Korn, T. M. (1961) *Mathematical Handbook for Scientists and Engineers.* McGraw-Hill, New York.

Mead, G. D. (1964) Deformation of the geomagnetic field by the solar wind. *J. geophys. Res.* 69, 1181.

Mead, G. D. and Beard, D. B. (1964) Shape of the geomagnetic field–solar wind boundary. *J. geophys. Res.* **69**, 1169.

Olson, W. P. (1969) The shape of the tilted magnetopause. *J. geophys. Res.* **74**, 5642.

Stern, D. P. (1985) Parabolic harmonics in magnetospheric modeling: the main dipole and the ring current. *J. geophys. Res.* **90**, 10851.

Tsyganenko, N. A. (1976) A model of cislunar magnetospheric field. *Ann. Geophys.* **32**, 1.

Voigt, G.-H. (1972) A three-dimensional analytical magnetospheric model with defined magnetopause. *Geophys. J.* **38**, 319.

Voigt, G.-H. (1981) A mathematical magnetospheric field model with independent physical parameters. *Planet Space Sci.* **29**, 1.